Developmental Analysis Reveals Mismatches in the Expression of K^+ Channel α Subunits and Voltage-gated K^+ Channel Currents in Rat Ventricular Myocytes

HAODONG XU,* JANE E. DIXON,‡ DIANNE M. BARRY,* JAMES S. TRIMMER,§ JOHN P. MERLIE,*† DAVID MCKINNON,‡ and JEANNE M. NERBONNE*

From the *Department of Molecular Biology and Pharmacology, Washington University, School of Medicine, St. Louis, Missouri 63110; ‡Department of Neurobiology and Behavior; and §Department of Cell Biology and Biochemistry, State University of New York at Stony Brook, Stony Brook, New York 11794-5215

ABSTRACT In the experiments here, the developmental expression of the functional Ca^{2+}-independent, depolarization-activated K^+ channel currents, I_{to} and I_K, and of the voltage-gated K^+ channel (Kv) α subunits, Kv1.2, Kv1.4, Kv1.5, Kv2.1, and Kv4.2 in rat ventricular myocytes were examined quantitatively. Using the whole-cell patch clamp recording method, the properties and the densities of I_{to} and I_K in ventricular myocytes isolated from postnatal day 5 (P5), 10 (P10), 15 (P15), 20 (P20), 25 (P25), 30 (P30), and adult (8–12 wk) rats were characterized and compared. These experiments revealed that mean I_{to} densities increase fourfold between birth and P30, whereas I_K densities vary only slightly. Neither the time- nor the voltage-dependent properties of the currents vary measurably, suggesting that the subunits underlying functional I_{to} and I_K channels are the same throughout postnatal development. In parallel experiments, the developmental expression of each of the voltage-gated K^+ channel α subunits, Kv1.2, Kv1.4, Kv1.5, Kv2.1, and Kv4.2, was examined quantitatively at the mRNA and protein levels using subunit-specific probes. RNase protection assays revealed that Kv1.4 message levels are high at birth, increase between P0 and P10, and subsequently decrease to very low levels in adult rat ventricles. The decrease in message is accompanied by a marked reduction in Kv1.4 protein, consistent with our previous suggestion that Kv1.4 does not contribute to the formation of functional K^+ channels in adult rat ventricular myocytes. In contrast to Kv1.4, the mRNA levels of Kv1.2, Kv1.5, Kv2.1, and Kv4.2 increase (three- to five-fold) between birth and adult. Western analyses, however, revealed that the expression patterns of these subunit proteins vary in distinct ways: Kv1.2 and Kv4.2, for example, increase between P5 and adult, whereas Kv1.5 remains constant and Kv2.1 decreases. Throughout development, therefore, there is a mismatch between the numbers of Kv α subunits expressed and the functional voltage-gated K^+ channel currents distinguished electrophysiologically in rat ventricular myocytes. Alternative experimental approaches will be required to define directly the Kv α subunits that underlie functional voltage-gated K^+ channels in these (and other) cells. In addition, the finding that Kv α subunit protein expression levels do not necessarily mirror mRNA levels suggests that caution should be exercised in attempting functional interpretations of observed changes in mRNA levels alone.

KEY WORDS: depolarization-activated K^+ channels • I_{to}, I_K • *Shaker, Shab, Shal* • Kv1.2, Kv1.4, Kv1.5, Kv2.1, Kv4.2

INTRODUCTION

Depolarization-activated outward K^+ currents contribute to determining the height and the duration of the plateau phase of the action potential in cardiac cells. In the mammalian myocardium, various types of depolarization-activated outward K^+ currents have been distinguished based on differences in time- and voltage-dependent properties and pharmacological sensitivities (Anumonwo et al., 1991; Varro et al., 1993; Barry and Nerbonne, 1996). In previous studies completed on adult rat ventricular myocytes, for example, transient (I_{to}) and delayed (I_K) type K^+ currents were distinguished based on differential sensitivities to 4-aminopyridine and tetraethylammonium (Apkon and Nerbonne, 1991). I_{to} and I_K also display markedly different time- and voltage-dependent properties, and functional studies revealed that these conductance pathways subserve distinct roles in action potential repolarization: I_{to} underlies the early phase of repolarization and is largely inactivated at later times, whereas I_K underlies the latter phase of repolarization back to the resting potential (Apkon and Nerbonne, 1991).

Interestingly, molecular cloning of cardiac K^+ channel pore-forming (α) subunits has revealed even greater potential for diversity than expected based on the numbers of depolarization-activated K^+ currents/channels distinguished electrophysiologically (Barry and Nerbonne, 1996). Five different voltage-gated K^+ channel (Kv) α subunits, for example, have been cloned from or shown to be expressed at the message level in

†Dr. Merlie died on May 27, 1995.

Address correspondence to Jeanne M. Nerbonne, Department of Molecular Biology and Pharmacology, Box 8103, Washington University School of Medicine, 660 South Euclid Avenue, Saint Louis, MO 63110; Fax: 314-362-7058; E-mail: jnerbonn@pharmdec.wustl.edu

adult rat heart; three of these (Kv1.2, Kv1.4, and Kv1.5) belong to the *Shaker* subfamily, one (Kv2.1) to the *Shab* subfamily, and one (Kv4.2) to the *Shal* subfamily (Tseng-Crank et al., 1990; Paulmichl et al., 1991; Roberds and Tamkun, 1991*a*; Dixon and McKinnon, 1994). There are, therefore, more Kv α subunits expressed than expected given that only two types of depolarization-activated K^+ channels have been distinguished electrophysiologically in adult rat ventricular myocytes (Apkon and Nerbonne, 1991). This discrepancy raises the interesting questions of what are the functional roles of the various Kv α subunits and, specifically, what underlies I_{to} and I_K? Recently, we exploited K^+ channel subunit-specific antibodies to examine the distributions of Kv1.2, Kv1.4, Kv1.5, Kv2.1, and Kv4.2 in adult rat heart. Immunohistochemistry and Western analysis revealed that Kv1.2, Kv1.5, Kv2.1, and Kv4.2 are readily detected in adult rat ventricular myocytes (Barry et al., 1995). Kv1.4, in contrast, was barely detectable, suggesting that this subunit does not contribute to the formation of I_{to} or I_K in these cells (Barry et al., 1995). Based on the relative distributions of Kv1.2, Kv1.5, Kv2.1, and Kv4.2 and on the properties of the K^+ channels formed on heterologous expression of these subunits, we suggested that Kv4.2 likely underlies rat ventricular I_{to} (Dixon and McKinnon, 1994; Barry et al., 1995) and that Kv2.1 underlies I_K (Barry et al., 1995).

The experiments here were undertaken to examine quantitatively the developmental expression of I_{to} and I_K and of the Kv α subunits, Kv1.2, Kv1.4, Kv1.5, Kv2.1, and Kv4.2 in rat ventricular myocytes at the mRNA and protein levels and to provide further insights into the relationship between these subunits and the functional K^+ channels in these cells. The electrophysiological studies revealed that I_{to} and I_K are the only K^+ currents expressed in ≥postnatal day 5 (P5)[1] rat ventricular myocytes and that these two conductance pathways develop independently. Although I_{to} densities increase severalfold between P5 and adult, the properties of I_{to} and I_K do not change appreciably as a function of age, suggesting that the subunits underlying functional I_{to} and I_K channels are the same throughout development. RNase protection assays revealed that Kv1.2, Kv1.5, Kv2.1, and Kv4.2 mRNA levels all increase (in parallel) during postnatal development. Western analyses, however, revealed that the developmental expression patterns of the corresponding subunit proteins are distinct. The levels of the Kv1.2 and Kv4.2 proteins, for example, increase with age, whereas Kv2.1 decreases, and Kv1.5 is invariant. The mismatch between the number of Kv α subunits and functional voltage-gated K^+ channels expressed in rat ventricular myocytes and the functional implications of this mismatch are discussed.

METHODS AND MATERIALS

Preparation of Isolated Myocytes

Ventricular myocytes were isolated from postnatal Long Evans rats of various ages using previously described procedures (Apkon and Nerbonne, 1991; Boyle and Nerbonne, 1991, 1992). Briefly, hearts were excised from anesthetized (5% halothane: 95% O_2) postnatal day 5 (P5), 10 (P10), 15 (P15), 20 (P20), 25 (P25), 30 (P30), and adult (8–12 wk) rats, mounted on a Langendorf perfusion apparatus, and perfused retrogradely through the aorta with 50 ml of a nominally Ca^{2+}-free HEPES-buffered Earles Balanced Salt solution (Gibco BRL, Gaithersburg, MD) supplemented with 6 mM glucose, amino acids, and vitamins (Buffer A). The quality of the perfusion was evidenced by the rapid clearing of blood from the coronary vessels. Hearts were then perfused with 50 ml of Buffer A containing 0.2–0.8 mg/ml collagenase B (Boehringer Mannheim Biochemicals, Indianapolis, IN) and 10 μM $CaCl_2$, and the flow rate was monitored continuously; the temperatures of the tissue and the perfusate were maintained at 34–35°C. The enzyme solution was filtered (at 5 μm) and recirculated through the heart until the flow rate doubled from its initial value (12–20 min); the lower two-thirds of the left and right ventricles were then removed and minced in the enzyme-containing Buffer A. The tissue pieces were transferred to fresh (enzyme-free) Buffer A supplemented with 1.25 mg/ml taurine, 5 mg/ml BSA (Sigma Chemical Co., St. Louis, MO), and 150 μM $CaCl_2$ (Buffer B) and then mechanically dispersed by gentle trituration. The resulting suspension was filtered to remove large undissociated tissue fragments, and isolated cells were obtained by sedimentation. The supernatant was discarded, and the cells were resuspended in Buffer B; this step was repeated twice to separate healthy cells from cellular fragments and debris. Isolated myocytes were resuspended in fresh Buffer B, plated on laminin-coated coverslips, and placed in a 95% air/5% CO_2 incubator at 37°C. Approximately 15 min after plating, serum-free medium-199 (M-199; Irvine Scientific, Santa Ana, CA), supplemented with antibiotics (penicillin/streptomycin), was added. Ca^{2+}-tolerant ventricular myocytes adhered preferentially to the laminin substrate, and damaged cells were easily removed by replacing the medium with fresh M-199 ~1 h after plating. Cells were examined electrophysiologically within 48 h of isolation.

Electrophysiological Recordings

The conventional whole-cell gigaohm seal recording technique (Hamill et al., 1981) was used to record Ca^{2+}-independent, depolarization-activated K^+ currents from isolated ventricular myocytes. Electrophysiological recordings were only obtained from Ca^{2+}-tolerant, rod-shaped ventricular cells, and all recordings were conducted at room temperature (22–24°C). The bath solution routinely contained (in mM): 136 NaCl, 4 KCl, 1 $CaCl_2$, 2 $MgCl_2$, 5 $CoCl_2$, 10 HEPES, 0.02 Tetrodotoxin, and 10 glucose at pH = 7.35 and 295–305 mOsm. Recording pipettes routinely contained (in mM): 135 KCl, 10 EGTA, 10 HEPES, 5 glucose, 3 K_2ATP, and 0.5 Tris-GTP at pH = 7.2 and 300–310 mOsm. β-Dendrotoxin (β-DTX; Alamone Labs, Jerusalem, Israel) and 4-aminopyridine (4-AP; Sigma Chemical Co.) stock solutions were prepared in distilled water and subsequently diluted to the appropriate concentration in bath solution immediately before the start of the experiments. Tetraethylammonium (TEA; Sigma)-containing bath solutions were prepared by equimolar substitution of TEACl for NaCl in the standard bath solution. β-DTX,

[1] *Abbreviations used in this paper:* DTX, dendrotoxin; HP, holding potential; P, postnatal day; TEA, tetraethylammonium; 4-AP, 4-aminopyridine.

4-AP, or TEA was applied to isolated myocytes during recordings using narrow-bore capillary tubes (inner diameter 300 μm) placed within 200 μm of the cell. The effects of β-DTX, 4-AP, or TEA were determined by comparing the currents in the presence of these agents with those of the currents recorded in the same cell during continuous superfusion of control bath solution.

Experiments were conducted using an Axopatch-1D amplifier (β = 1) (Axon Instruments, Foster City, CA). Recording pipettes, fabricated from soda lime glass, had tip diameters of 2–3 μm and resistances of 2–4 MΩ when filled with recording solution; seal resistances were ≥5 GΩ. After establishing the whole-cell configuration, ±10 mV steps were applied to allow measurements of cell membrane capacitances and input resistances. Whole-cell membrane capacitances and series resistance were compensated (≥85%) electronically; voltage errors resulting from the uncompensated series resistance were always ≤7 mV and were not corrected. Depolarization-activated K^+ currents were routinely evoked during voltage steps to potentials between −40 and +50 mV from a holding potential (HP) of −70 mV; voltage steps were presented in 10-mV increments at 5-s intervals. Experiments were controlled, and data were acquired using a Northgate 486 (33 MHz) microcomputer equipped with a Tecmar Labmaster (Scientific Solutions) analogue/digital interface and the pClamp 5.5 software package (Axon Instruments). Data were acquired at 5–12.5 kHz, and current signals were filtered at 5 kHz before digitization and storage.

Data Analysis

Analyses of digitized data were completed using pClamp 5.5. Whole-cell membrane capacitances were determined by integrating the capacitative transients evoked during ±10-mV voltage steps from an HP of −70 mV (before using the feedback circuit for series resistance and capacity compensation). Mean (±SD) cell membrane capacitance increased from 28.8 ± 8.4 pF (n = 9) in P5 cells to 124.6 ± 17.8 (n = 13) in adult cells. Input resistances, in contrast, did not vary appreciably as a function of the age of the animal from which the cells were isolated. The mean ± SEM input resistances for P5 (n = 9), P10 (n = 7), P15 (n = 14), P20 (n = 9), P25 (n = 10), P30 (n = 9), and adult (n = 13) were 1.31 ± 0.30, 1.05 ± 0.12, 1.39 ± 0.21, 1.32 ± 0.25, 1.42 ± 0.27, 1.23 ± 0.20, and 1.02 ± 0.16 GΩ, respectively. The mean ± SEM input resistance for all cells was 1.26 ± 0.08 GΩ (n = 71). Leak currents in all cells, therefore, were negligible and were not corrected. Peak currents at each test potential were measured as the difference between the maximal outward current amplitudes and the zero current level. Plateau currents were measured as the difference between the outward current amplitudes remaining 140 ms after the onset of depolarizing voltage steps and the zero current level.

The waveforms of the 4-aminopyridine (4-AP)-, tetraethylammonium (TEA)-, or β-dendrotoxin (β-DTX)-sensitive currents were determined by subtraction of the currents measured in the presence of 4-AP, TEA, or β-DTX from those measured in control bath solution. Activation and inactivation time constants were determined from single exponential fits to the rising and decaying phases, respectively, of the currents evoked during membrane depolarizations. For analyses of the activation rates, the rising phases of the currents were fit from the onset of the outward current (after the initial delay) to the peak; for analyses of inactivation rates, the zero time was set at the peak of the outward current. Correlation coefficients (R) were determined to assess the quality of fits; R values for the fits included in the analyses here were in the range of 0.94 to 0.99. All averaged and normalized data are presented as means ± SEM). The statistical significance of apparent differences between different populations of cells was assessed using the analyses of variance (ANOVA) or the Student's t test; P values are presented in the text and significance was set at the $P < 0.05$ level.

Preparation of RNA from Rat Ventricles

RNA samples were pooled from dissections of the lower two-thirds of total ventricle from Long Evans rats ranging from birth (day 0) to young adult (8–12 wk; ~200 g). Animals were anesthetized, the chest cavity was opened, and the heart was removed. Hearts were then transected below the major vessels, and the lower two-thirds, including both the left and right ventricles, were removed. Tissue samples were first blotted on paper towels to remove excess blood and then quickly frozen in liquid N_2. Frozen tissue samples were homogenized in guanidinium thiocyanate and total RNA was prepared by pelleting over a CsCl step gradient. All RNA samples were quantified by spectrophotometric analyses, and the integrity of each RNA sample was confirmed by analysis on a denaturing agarose gel (Dixon and McKinnon, 1994).

RNase Protection Assays

DNA templates for the preparation of RNA probes were prepared as described previously (Dixon and McKinnon, 1994). In all cases, a substantial amount of nonhybridizing sequence (~50 basepairs) was included in the probe to allow easy distinction between the probe and the specific protected band. Probe sequences were selected such that no probe had long uninterrupted regions of identity with any known transcript other than the transcript to be tested. Because of the inherent specificity of the RNase protection assay, there was no evidence for unwanted cross-reaction between the probe and a nonspecific potassium channel subunit transcript. RNase protection assays were performed as described previously (Dixon and McKinnon, 1994). For each sample point, 10 μg of RNA was used in the assay. A probe for the rat cyclophilin gene (Danielson et al., 1988) was obtained and used in the hybridization as an internal control to confirm that part of the sample was not lost or degraded during the assay. 5 μg of yeast tRNA was used as a negative control to test for the presence of probe self protection bands. RNA expression was quantified directly from the gels using a Betascope 603 (Biogenics, San Ramon, CA). Mean ± SEM data from four to seven independent determinations are presented.

Membrane Preparations

Ventricular membranes were prepared from the hearts of Long Evans rats isolated at P5, P10, P15, P20, P25, P30, and adult (8–12 wk) using a previously described protocol (Barry et al., 1995). Briefly, animals were anesthetized with 5% halothane/ 95% O_2, the chest cavity was opened, and the heart was removed. Hearts were then transected below the major vessels; the lower half from the apex, including both the left and right ventricles, was removed, rinsed in 10 mM PBS at 4°C, and frozen at −70°C. All procedures were performed at 4°C, and all solutions contained the following protease inhibitors: 1 mM iodoacetamide, 1 mM 1,10 phenanthroline, 2 μg/ml aprotinin, 1 mM benzamidine, 1 μg/ml pepstatin, and 0.5 mM pefebloc. Ventricles were minced, diluted in 10 volumes of 10 mM Tris and 1 mM EDTA buffer (TE) at pH = 7.4, and homogenized using a polytron (Brinkman Instruments, Inc., Westbury, NY). Nuclei and debris were pelleted by centrifugation at 1,000 g for 10 min. This procedure was repeated, and the supernatants from both low speed spins were pooled and centrifuged at 40,000 g for 10 min. Pellets were resuspended in TE containing 0.6 M KI and incubated on ice for 10 min. After centrifuging at 40,000 g for 10 min, the resulting pellets were resuspended in TE and centrifuged again at 40,000 g. To ensure that the KI was removed, this step was repeated. The fi-

nal pellets were solubilized in TE and 2% Triton X-100 on ice for 1 h. Insoluble material was centrifuged at 13,000 *g* for 10 min. The protein content of each of the solubilized membrane preparations was determined using a protein assay kit (Bio-Rad Laboratories, Richmond, CA). Solubilized membranes were aliquoted and stored frozen at −20°C until used.

Western Blots

For immunoblots, ventricular membrane proteins (20 μg) were added to reducing SDS sample buffer, boiled, and fractionated on 10% polyacrylamide gels. To facilitate quantitative comparisons of the expression patterns of the Kv α subunits, membrane proteins (20 μg) prepared from P5, P10, P15, P20, P25, P30, and adult rat ventricles were loaded onto the same gel. After separation, membrane proteins were electrophoretically transferred to PVDF membranes (DuPont, Wilmington, DE or Amersham Corp., Arlington Heights, IL), and subsequently probed with antibodies directed against Kv1.2 (Sheng et al., 1993, 1994), Kv1.4 (Sheng et al., 1992, 1993), Kv1.5 (Takimoto and Levitan, 1994; Maletic-Savatic et al., 1995), Kv2.1 (Trimmer, 1991), or Kv4.2 (Sheng et al., 1992, 1993), as described previously (Barry et al., 1995). The membranes were blocked in PBS containing 0.2% I-Block (Tropix, Bedford, MA) in PBS containing 0.1% Tween 20 for 1 h at room temperature and incubated overnight at 4°C in primary antibody solution prepared in PBS containing 5% normal goat serum, 0.2% Triton X-100, and 0.1% NaN_3. After incubation in the primary antibody, membranes were washed two times in blocking buffer for 10 min, and subsequently incubated in alkaline phosphatase–conjugated goat-anti–rabbit IgG (Tropix) diluted 1:10,000 in blocking buffer for 1 and one-half hours at room temperature, and then washed three times in blocking buffer and twice in Assay Buffer (Tropix; 0.1 M DEA and 1 mM $MgCl_2$) for 40 min total. Bound antibodies were detected using the CPSD (Tropix) chemiluminescent alkaline phosphatase substrate.

Films of Western blots were scanned into a Molecular Dynamics Personal Densitometer using Image Quant (Molecular Dynamics, Inc., Sunnyvale, CA). The density of each band was quantified by summing the pixel values above the background within a defined area surrounding the band. Each density value was then normalized to the density determined for the band in the adult sample on the same gel. For the Kv2.1 blots, only the higher molecular weight band (at 130 kD) was included in the analyses. Mean (±SEM) values from three to six independent determinations are presented.

RESULTS

Developmental Expression of Outward K^+ Currents in Ventricular Myocytes

To examine the developmental expression of the Ca^{2+}-independent, depolarization-activated outward K^+ currents, ventricular myocytes were isolated from postnatal day 5 (P5), 10 (P10), 15 (P15), 20 (P20), 25, (P25), 30 (P30), and adult rat hearts. Using the described procedures (see MATERIALS AND METHODS), 50–90% of the ventricular myocytes isolated from animals of all ages were rod-shaped and had clear cross striations; electrophysiological recordings were obtained only from Ca^{2+}-tolerant rod-shaped cells, and, in general, smaller cells were selected for recordings to ensure the fidelity of the voltage-clamp recordings. Visual inspection did reveal, however, that there are clear differences in the sizes of cells isolated at different ages. In particular, ventricular myocytes isolated at P5–P15 appeared substantially smaller and more spindle-shaped than cells isolated from older (≥P20) animals. Similar morphological differences in rat ventricular myocytes isolated at various postnatal ages have been described recently by Wahler and colleagues (1994). In the presence of TTX (20 μM) and Co^{2+} (5 mM) to block inward Na^+

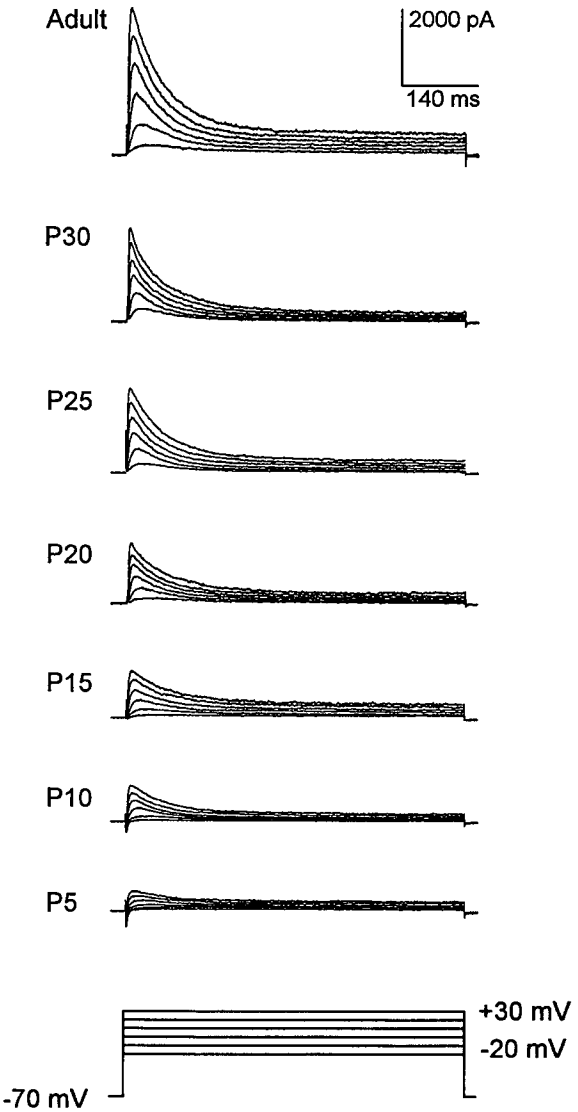

FIGURE 1. Waveforms of the Ca^{2+}-independent, depolarization-activated K^+ currents in ventricular myocytes isolated from adult, and from postnatal day 30 (P30), 25 (P25), 20 (P20), 15 (P15), 10 (P10), and 5 (P5) rat hearts. Currents, recorded using the whole-cell patch-clamp technique, were evoked during 625-ms depolarizing voltage steps to test potentials between −20 mV and +30 mV from an HP of −70 mV. Depolarizing voltage steps were presented in 10-mV increments at 5-s intervals. The bath contained 20 μM TTX and 5 mM Co^{2+} to suppress inward Na^+ and Ca^{2+} currents, respectively.

and Ca^{2+} currents, respectively, depolarization-activated outward K^+ currents were routinely recorded during depolarizations to potentials between −40 and +50 mV from an HP of −70 mV. Typical outward K^+ current waveforms recorded from cells isolated at various developmental ages are displayed in Fig. 1. As is evident, outward K^+ current amplitudes increase markedly from P5 to adult, and the peak outward currents increase to a greater extent than the plateau currents as a function of postnatal age (Fig. 2 *A*). The (mean ± SEM) peak current amplitude evoked at +30 mV from an HP of −70 mV, for example, increased more than sevenfold from 346 ± 52 (n = 9) at P5 to 2,484 ± 212 pA (n = 9) at P30. Mean (±SEM) plateau current amplitudes evoked at +30 mV from an HP of −70 mV, in contrast, increased threefold during the same developmental period from 194 ± 32 (n = 9) at P5 to 618 ± 37 pA (n = 9) at P30. Both the peak and the plateau current amplitudes increased progressively throughout postnatal development (Fig. 2 *A*).

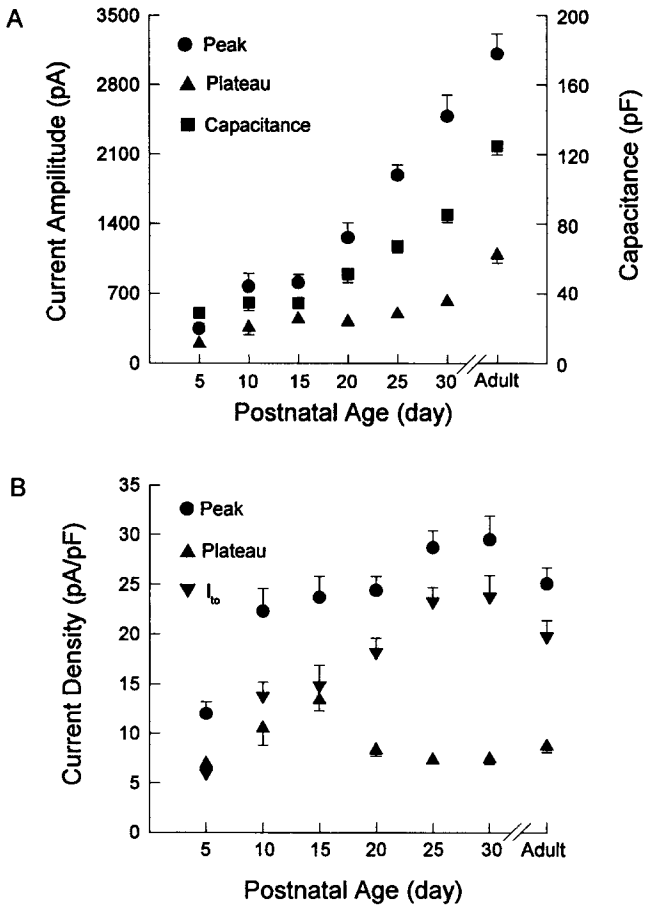

FIGURE 2. Variations in whole-cell membrane capacitances (*A*), peak and plateau outward current amplitudes (*A*) and densities (*B*) in ventricular myocytes isolated from P5 (n = 9), P10 (n = 7), P15 (n = 14), P20 (n = 9), P25 (n = 10), P30 (n = 9), and adult (n = 13) animals. (*A*) Whole-cell membrane capacitances (■) were determined by integrating the capacitative transients evoked during ±10-mV voltage steps from an HP of −70 mV; mean ± SEM values are plotted as a function of age. Outward currents were recorded as described in the legend of Fig. 1. Peak and plateau currents evoked at +30 mV from a HP of −70 mV were measured in individual cells, and mean ± SEM values for the peak (●) and the plateau (▲) current amplitudes are plotted as a function of postnatal age. (*B*) Peak and plateau current densities were determined in individual cells by dividing the (peak and plateau) current amplitudes by the whole cell membrane capacitance (of the same cell); mean ± SEM values for the peak (●) and plateau (▲) current densities are plotted as a function of postnatal age. I_{to} amplitudes were determined from single exponential fits to the rapid decay phases of the currents evoked at +30 mV from an HP of −70 mV, and I_{to} densities in individual cells were determined by dividing the measured current amplitude by the whole cell membrane capacitance; mean ± SEM I_{to} densities (▼) are plotted as a function of postnatal age.

As noted above, ventricular myocytes isolated from early (≤P15) postnatal animals appeared smaller than those isolated from older (≥P20) animals. Examination of whole-cell membrane capacitances confirmed substantial differences in cell size as a function of age: mean (±SEM) whole-cell membrane capacitance increased significantly ($P < 0.001$, ANOVA) from 28.8 ± 2.8 pF (n = 9) at P5 to 124.6 ± 4.9 pF (n = 13) for adult cells (Fig. 2 *A*). To facilitate comparisons between cells of different sizes, peak and plateau current amplitudes in each cell were measured and normalized to the whole-cell membrane capacitance (of that cell). There was no correlation between cell size (as assessed by the whole-cell membrane capacitance) and the peak or plateau current density. Mean (±SEM) peak and plateau outward current densities are plotted in Fig. 2 *B*. Peak current densities increase significantly (ANOVA, $P < 0.01$) from 12.0 ± 1.2 (n = 9) in P5 cells to 28.7 ± 1.7 pA/pF (n = 10) in P25 cells; peak outward current densities did not change appreciably between P25 and adult. Plateau current densities, in contrast, increased slightly from 6.9 ± 0.7 (n = 9) at P5 to 13.4 ± 1.1 pA/pF (n = 14) at P15 and then decreased again to 7.3 ± 0.3 pA/pF (n = 10) at P25; no further changes in plateau current densities were evident in cells isolated at times later than P25 (Fig. 2 *B*). The increase in plateau current density between P5 and P15 is statistically significant ($P < 0.01$), as is the decrease in plateau current density between P15 and P25. Interestingly, however, plateau current densities are not significantly (Student's t test) different in P5 and adult rat ventricular myocytes (Fig. 2 *B*).

Previously, we demonstrated that the total Ca^{2+}-independent, depolarization-activated outward K^+ currents in adult rat ventricular myocytes reflect the activation of two distinct K^+ current components, I_{to} and I_K (Apkon and Nerbonne, 1991). In adult rat ventricular myocytes, the peak outward current amplitudes evoked during depolarizing voltage steps largely reflect the activation of I_{to}, whereas I_K underlies the plateau currents

(Apkon and Nerbonne, 1991). In addition, the rapidly decaying component of the total outward current reflects I_{to} exclusively, uncontaminated by I_K (Apkon and Nerbonne, 1991). In adult cells, therefore, determination of the amplitudes of the rapidly decaying current component in records such as those in Fig. 1 provides a direct way to estimate I_{to} amplitudes (densities). Assuming that this would also be the case in cells isolated at P5 through P30 (if the properties of I_{to} were unchanged as a function of postnatal age), the decay phases of the currents evoked at +30 mV from an HP of −70 mV were analyzed. These analyses revealed that I_{to} amplitudes and densities increase markedly as a function of age: mean ± SEM I_{to} densities increased from 6.0 ± 0.8 (n = 9) at P5 to 23.8 ± 2.1 pA/pF (n = 9) at P30 (Fig. 2 *B*). These results support the hypothesis that the rapidly decaying component of the currents indeed reflects I_{to} at all ages, and, in addition, suggest that the time- and voltage-dependent properties of this component do not change appreciably during development. Subsequent experiments, therefore, were focussed on examining the time- and voltage-dependent properties of the currents in greater detail.

To determine the voltage dependences of activation of the currents in developing and adult rat ventricular myocytes, the peak and plateau amplitudes of the currents evoked during depolarizations to test potentials between −40 and +30 mV from an HP of −70 mV were measured in individual cells and subsequently normalized to their respective (peak and plateau) amplitudes recorded during depolarization to +30 mV (in the same cell). Mean (±SEM) normalized peak and plateau current amplitudes determined in P5 and adult rat ventricular myocytes are plotted in Fig. 3. The normalized current-voltage relations for the peak (I_{to}) and the plateau (I_K) currents in P5 (n = 5) and adult (n = 10) cells are indistinguishable (Fig. 3). Similar results were obtained when cells isolated from P10 (n = 7), P15 (n = 14), P20 (n = 10), P25 (n = 10), and P30 (n = 9) were examined (not illustrated). To determine the voltage dependences of steady-state inactivation of the currents in P10 and P20 myocytes, currents were evoked at +30 mV from various holding potentials (−120 to 0 mV). Peak and plateau currents were measured, normalized to their respective amplitudes for currents evoked from −120 mV, and plotted as a function of prepulse (holding) potential. Similar to our previous findings in adult cells (Apkon and Nerbonne, 1991), inactivation of the peak currents in P10 and P20 myocytes is well described by the sum of two Boltzmanns (reflecting contributions from both I_{to} and I_K, the latter only at hyperpolarized prepulse potentials), whereas the plateau current is well described by a single Boltzmann (corresponding to inactivation of I_K). In P20 cells (n = 4), the $V_{1/2}$ values for the peak currents were −78 mV (k = 12.4) and −28 mV (k = 4.8). In P10 cells (n = 4), the best double Boltzmann fit to the data points yielded $V_{1/2}$ values of −78 mV (k = 8.9) and −33 mV (k = 5.8). These values are nearly identical to those obtained on adult cells where $V_{1/2}$ values of −77 mV (k = 12.9) and −29 mV (k = 5.5) were obtained (Apkon and Nerbonne, 1991). Changes in the voltage dependences of activation and/or inactivation of the currents, therefore, cannot account for the increases in current amplitudes and densities observed during postnatal development (Fig. 2 *B*).

Similar to our findings in adult myocytes, we found that I_{to} in postnatal cells is selectively blocked by 4-aminopyridine (4-AP). Typical effects of 0.5 mM 4-AP (which blocks ~50% of the peak current [and I_{to}]) (Castle and Slawsky, 1992) are displayed in Fig. 4. At all ages, 0.5 mM 4-AP selectively attenuates the peak outward currents and is without effects on the plateau currents. The amplitudes of the 4-AP-sensitive currents (Fig. 4 *C*), obtained by subtraction of the currents recorded in the presence of 0.5 mM 4-AP (Fig. 4 *B*) from the controls (Fig. 4 *A*), increase markedly between P5 and P30; the mean (±SEM) amplitude of the current sensitive to 0.5 mM 4-AP increased significantly (P < 0.001, ANOVA) from 109 ± 32 (n = 4) at P5 to 1,886 ± 233 pA (n = 7) at P30. Even taking into account the large change in cell size observed during postnatal development, the mean (±SEM) 0.5 mM 4-AP-sensitive

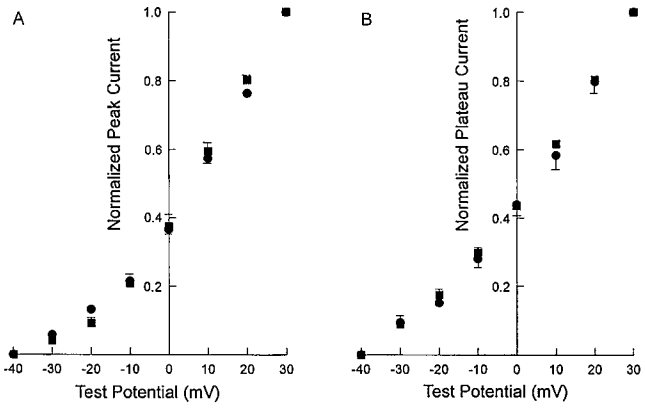

FIGURE 3. The voltage dependences of activation of the peak and the plateau currents do not vary measurably during postnatal development. Outward K^+ currents were evoked during 140-ms depolarizations to potentials between −40 mV and +60 mV from an HP of −70 mV as described in the legend of Fig. 1. For each cell, the amplitudes of the peak and plateau currents were measured at each potential and normalized to their respective (peak and plateau) amplitudes evoked (in the same cell) at +30 mV. Mean (±SEM) normalized peak (*A*) and plateau (*B*) outward current amplitudes determined for ventricular myocytes isolated from P5 (●) (n = 9) and adult (■) (n = 13) animals are plotted as a function of test potential. Similar results were obtained for cells isolated at P10 (n = 7), P15 (n = 14), P20 (n = 10), P25 (n = 10), and P30 (n = 9).

current density increased significantly ($P < 0.001$, ANOVA) from 2.8 ± 0.8 pA/pF ($n = 4$) at P5 to 18.4 ± 2.0 pA/pF ($n = 7$) at P30.

Qualitatively, the waveforms of the total depolarization-activated outward K^+ currents (Figs. 1 and 4 *A*) and the 0.5 mM 4-AP–sensitive currents (Fig. 4 *C*) appear similar at all developmental ages. To determine the kinetic properties of the currents, time constants (tau) for activation and inactivation of the peak outward currents were determined from single exponential fits to the rising and decaying phases, respectively, of the total outward currents. Activation and inactivation of the peak outward currents in adult rat ventricular myocytes are dominated by I_{to} (Apkon and Nerbonne, 1991). Analyzing these rates, therefore, gives reliable estimates of the kinetics of I_{to} activation and inactivation (Apkon and Nerbonne, 1991). As reported previously (Apkon and Nerbonne, 1991), the time constants for activation of the peak currents in adult cells are voltage dependent, decreasing with increasing depolarization (Table I). Similar voltage dependences were seen at all developmental stages studied (Table I). These analyses also revealed that the time constants for peak outward current activation are invariant between P10 and adult (Table I). In P5 cells, however, the activation time constants, although clearly also voltage dependent, are approximately twofold longer than those determined in ≥P10 cells. Although the differences between the activation time constants in P5 and ≥P10 are small, they are statistically significant ($P < 0.01$, ANOVA). Because of the small amplitudes of the currents, particularly I_{to}, in P5 cells (Fig. 4), it seemed likely that the peak outward currents (and, therefore, the activation of the peak currents) might be contaminated by the presence and the activation of I_K. To provide an independent measure of I_{to} activation rates, therefore, the rising phases of the 0.5 mM 4-AP–sensitive currents (in subtracted records such as those in Fig. 4 *C*) were also analyzed. These analyses revealed time constants for I_{to} activation in P5 cells ($n = 4$) that are not significantly (ANOVA) different from the activation time constants determined for P10 to adult cells, suggesting that the slower activation of the total outward currents determined in P5 cells reflect contamination from the slower activating I_K. The rising phases of the total outward currents in P10 through adult cells, in contrast, are dominated by activation of I_{to}.

The time constants for inactivation of the peak outward currents were determined from single exponential fits to the decay phases of the total outward currents. These analyses revealed that inactivation is voltage independent (Table II) and that there are no significant differences in the inactivation time constants in cells isolated at various stages of development

TABLE I

Time Constants of Peak Outward Current Activation in Rat Ventricular Myocytes as a Function of Postnatal Age

Age	Activation Tau (ms)				
	−10 mV	0 mV	+10 mV	+20 mV	+30 mV
P5	20.1 ± 5.0 ($n = 3$)	11.2 ± 1.1 ($n = 5$)	5.1 ± 0.9 ($n = 5$)	3.5 ± 0.4 ($n = 5$)	2.6 ± 0.4 ($n = 5$)
P10	12.6 ± 3.6 ($n = 7$)	5.1 ± 0.6 ($n = 7$)	3.4 ± 0.5 ($n = 7$)	2.4 ± 0.2 ($n = 7$)	1.7 ± 0.1 ($n = 7$)
P15	10.2 ± 1.7 ($n = 6$)	6.7 ± 0.7 ($n = 7$)	4.0 ± 0.6 ($n = 7$)	2.3 ± 0.6 ($n = 7$)	1.6 ± 0.7 ($n = 7$)
P20	8.3 ± 1.8 ($n = 8$)	4.7 ± 0.7 ($n = 9$)	2.9 ± 0.3 ($n = 9$)	1.6 ± 0.2 ($n = 9$)	1.5 ± 0.3 ($n = 9$)
P25	8.0 ± 0.9 ($n = 10$)	5.2 ± 0.9 ($n = 10$)	3.5 ± 0.5 ($n = 10$)	2.2 ± 0.4 ($n = 10$)	1.5 ± 0.3 ($n = 10$)
P30	6.9 ± 0.7 ($n = 8$)	4.1 ± 0.4 ($n = 9$)	2.6 ± 0.4 ($n = 9$)	1.6 ± 0.2 ($n = 9$)	1.1 ± 0.2 ($n = 9$)
Adult	8.5 ± 1.4 ($n = 8$)	5.2 ± 0.7 ($n = 8$)	3.2 ± 0.4 ($n = 8$)	1.9 ± 0.2 ($n = 8$)	1.4 ± 0.1 ($n = 8$)

Values are means ± SEM. Time constants for outward current activation in individual cells were determined from single exponential fits to the rising phases of the total outward currents evoked at potentials between −10 and +30 mV from an HP of −70 mV.

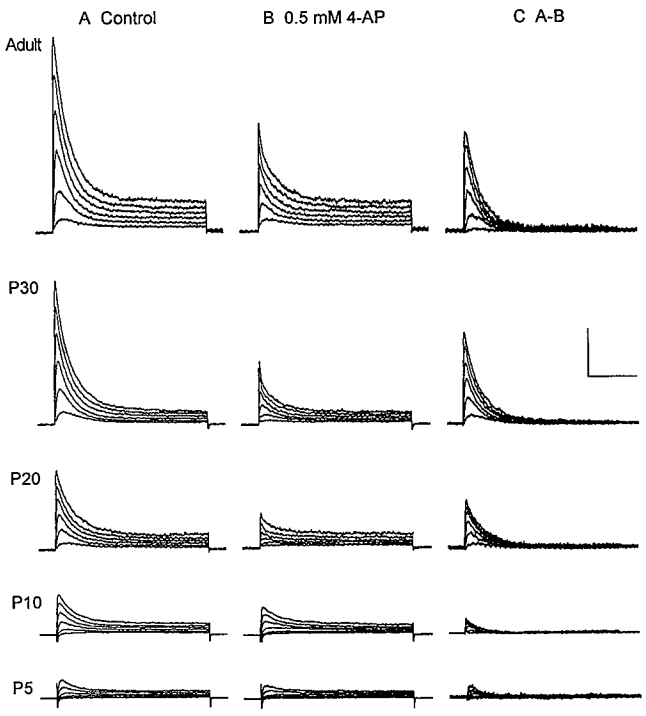

FIGURE 4. The amplitudes of the 4-AP–sensitive transient outward currents (I_{to}) increase markedly during postnatal development. Currents were recorded from rat ventricular myocytes isolated at various ages as described in the legend of Fig. 1 under control conditions (*A*) and after exposure to 0.5 mM 4-AP. The currents recorded in the presence of 4-AP are plotted in *B*. The 4-AP–sensitive currents, plotted in *C*, were obtained by subtraction of the records in 0.5 mM 4-AP (*B*) from those recorded in control bath solution (*A*). Scale bars are 1,000 pA and 200 ms.

TABLE II

Time Constants of Peak Outward Current Inactivation in Rat Ventricular Myocytes as a Function of Postnatal Age

	Inactivation Tau (ms)			
Age	0 mV	+10 mV	+20 mV	+30 mV
P5	63.4 ± 8.4 (n = 4)	54.1 ± 5.4 (n = 4)	61.2 ± 7.7 (n = 4)	59.9 ± 6.4 (n = 4)
P10	57.6 ± 3.0 (n = 7)	55.3 ± 2.5 (n = 7)	60.2 ± 2.9 (n = 7)	64.1 ± 1.2 (n = 7)
P15	57.6 ± 5.8 (n = 7)	55.3 ± 2.5 (n = 7)	58.1 ± 2.5 (n = 7)	61.5 ± 3.0 (n = 7)
P20	54.2 ± 5.4 (n = 9)	53.4 ± 3.0 (n = 9)	52.8 ± 3.4 (n = 9)	56.1 ± 3.8 (n = 9)
P25	50.2 ± 2.5 (n = 10)	48.3 ± 1.2 (n = 10)	51.4 ± 1.5 (n = 10)	54.6 ± 1.9 (n = 10)
P30	56.1 ± 3.5 (n = 9)	53.7 ± 1.2 (n = 9)	55.1 ± 1.5 (n = 9)	58.9 ± 1.2 (n = 9)
Adult	50.9 ± 2.8 (n = 8)	51.5 ± 1.8 (n = 8)	54.3 ± 1.7 (n = 8)	57.5 ± 2.1 (n = 8)

Values are means ± SEM. Time constants for outward current inactivation in individual cells were determined from single exponential fits to the decay phases of the total outward currents evoked at potentials between 0 and +30 mV from an HP of −70 mV.

from P5 through adult (Table II). Inactivation time constants for I_{to}, determined from single exponential fits to the decaying phases of the 4-AP–sensitive currents in subtracted currents, were indistinguishable from those determined from analyses of the decay phases of the total currents. Taken together, these results confirm that the voltage-independent inactivation of I_{to} underlies the inactivation of the total outward currents. In addition, these experiments revealed that the time constants for I_{to} inactivation are the same at all stages of postnatal development, from P5 through the adult. The finding that I_{to} inactivation rates are invariant during postnatal development validates the analyses above of the rapidly decaying component of the total outward currents as a way to estimate I_{to} amplitudes (densities) as a function of postnatal age.

In adult rat ventricular myocytes, I_K is selectively blocked by mM concentrations of TEA (Apkon and Nerbonne, 1991). To provide an independent way to assess whether the time-dependent properties of I_K vary during postnatal development, cells were exposed to TEA. The waveforms of the total depolarization-activated K^+ currents were recorded under control conditions and in the presence of 50 mM TEA. As reported previously (Apkon and Nerbonne, 1991), these experiments revealed that TEA selectively attenuates the plateau currents; there is little effect of TEA on the peak currents. The waveforms of the "TEA-sensitive" currents (Fig. 5) were then obtained by subtraction of the currents recorded in the presence of TEA from the controls. As illustrated if Fig. 5, the waveforms of the TEA-sensitive currents in P10 (Fig. 5 *A*), P20 (Fig. 5 *B*), and adult (Fig. 5 *C*) rat ventricular myocytes are indistinguishable. Taken together, therefore, the electrophysiological experiments suggest that neither the time- nor the voltage-dependent properties of I_{to} or I_K varies measurably during postnatal development.

Developmental Expression of Kv1.2, Kv1.5, Kv2.1, and Kv4.2 mRNAs

Previously, Dixon and McKinnon (1994) demonstrated that the mRNAs for voltage-gated K^+ channel α-subunits Kv1.2, Kv1.4, Kv1.5, Kv2.1, and Kv4.2 are readily detected in adult rat ventricular myocytes using quantitative RNase protection assays. To determine whether the expression patterns of these subunits vary during postnatal development, RNase protection assays were performed on samples prepared from P0, P5, P10, P16, P24, P30, and adult rat ventricles. These experiments revealed significant increases in Kv1.2, Kv1.5, Kv2.1, and Kv4.2 mRNA levels during postnatal development

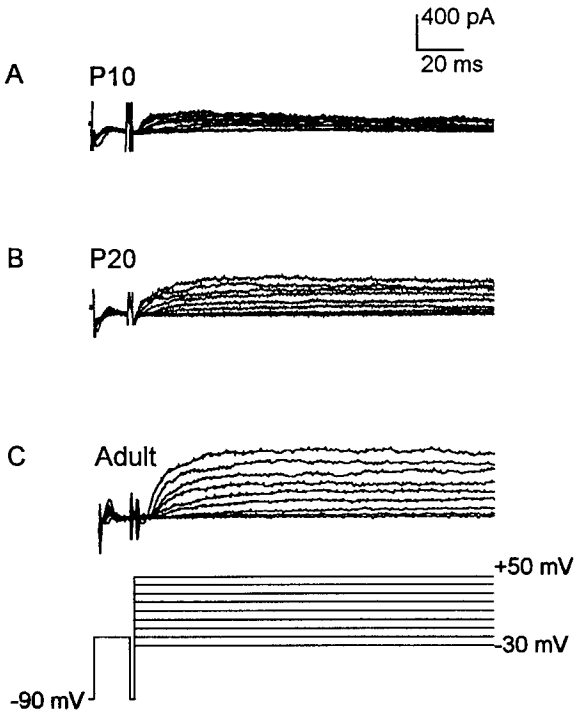

FIGURE 5. The waveforms of the TEA-sensitive outward currents (I_K) do not vary measurably during postnatal development. Outward currents were recorded during depolarizations to potentials between −30 and +50 mV from an HP of −90 mV; a 15-ms prepulse to −20 mV was delivered in each trial (see paradigm below the current records). Currents were recorded under control conditions and following bath application of 50 mM TEA; the waveforms of the TEA-sensitive currents were obtained by subtraction of the currents recorded in the presence of TEA from the controls. Illustrated are TEA-sensitive outward currents in rat ventricular myocytes isolated from P10 (*A*), P20 (*B*), and adult (*C*) animals.

(Fig. 6). The timing of the increases was similar for Kv1.2, Kv1.5, and Kv2.1 in that the largest (percent) increases were observed between P5 and P15. Overall, the largest changes were evident for Kv1.2 mRNA, which increases approximately 8 fold between birth and adult (Fig. 6, *upper left*). The Kv1.5 and Kv2.1 mRNAs showed smaller increases over the same time period (Fig. 6). For Kv4.2, there was also an increase between P5 and P15, but the increase was modest compared to that seen with Kv1.2, Kv1.5, and Kv2.1. There was a slightly more prominent increase in Kv4.2 mRNA between P20 and adult (Fig. 6, *lower right*). The observed increases in Kv1.2, Kv1.5, Kv2.1, and Kv4.2 mRNAs were not due to generalized increases in mRNA abundance, as evidenced by the fact that a marked decline in the abundance of Kv1.4 mRNA was observed: Kv1.4 mRNA peaked at P5–P10 and steadily declined during development (see below and Fig. 9).

Developmental Expression of Kv1.2, Kv1.5, Kv2.1, and Kv4.2 Proteins

Previously, we demonstrated that the voltage-gated K^+ channel α-subunits Kv1.2, Kv1.5, Kv2.1, and Kv4.2 (but not Kv1.4) are readily detected in adult rat ventricular myocyte membranes by immunohistochemistry and Western analysis (Barry et al., 1995). To determine whether the expression patterns of these subunits vary during postnatal development, Western blots were performed on membrane proteins prepared from P5, P10, P15, P20, P25, P30, and adult rat ventricles after fractionation on SDS polyacrylamide gels and transfer to PVDF membranes. To facilitate comparison of the expression levels of each of the subunits as a function of postnatal age, equal amounts of membrane proteins (20 μg) prepared at each age were loaded on the same gel for subsequent immunoblotting with one of the anti-Kv α subunit–specific antibodies. Typical results obtained using the antibodies against Kv1.2, Kv1.5, Kv2.1, and Kv4.2 are presented in Fig. 7. As is evident, the anti-Kv1.2 antibody recognizes a single, specific band at 75 kD in ventricular membranes (Fig. 7, *upper left*) at all ages; no labeling is seen in Western blots when the antibody was preincubated with the peptide against which the antibody was generated (Barry et al., 1995). As is also evident in Fig. 7, the amount of the Kv1.2 protein increases markedly as a function of age. Similar results were obtained in several experiments, and mean normalized data (see MATERIALS AND METHODS) are presented in Fig. 8 (*upper left*). The density of Kv1.2 increases approximately fourfold between P5 and P20 and then decreases slightly to its adult level. Interestingly, variations in the Kv1.2 protein (Figs. 7 and 8) parallel those seen for the Kv1.2 mRNA (Fig. 6).

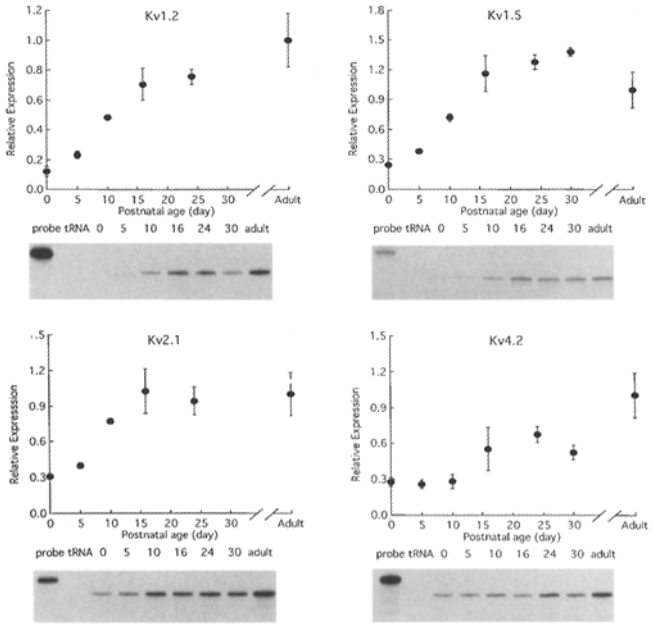

FIGURE 6. The expression levels of the messages for Kv1.2, Kv1.5, Kv2.1, and Kv4.2 in rat ventricles increase during postnatal development. The four panels show graphs of the relative changes in mRNA expression for Kv1.2 (*upper left*), Kv1.5 (*upper right*), Kv2.1 (*lower left*), and Kv4.2 (*lower right*). The data points plotted reflect the mean (±SEM) of four to seven independent determinations. Underneath each of the four graphs is shown a representative gel from an RNase protection assay using one of the subunit specific probes. For each assay, 10 μg of RNA was used; RNA expression was quantified directly from the gels. The data were normalized to the mean value for the adult sample in each experiment, which was set equal to unity.

In parallel experiments, Western blots of ventricular membrane proteins revealed that Kv1.5, Kv2.1, and Kv4.2 are also readily detected at all developmental ages (Fig. 7). The anti-Kv4.2 antibody specifically labels a single band at 74 kD in rat ventricular membranes at all developmental ages (Fig. 7, *lower right*). In addition, the labeling was eliminated when the anti-Kv4.2 antibody was preincubated with the peptide against which the antibody was generated (data not shown). Similar results were obtained in several experiments, and mean normalized data for Kv4.2 expression are presented in Fig. 8 (*lower right*). Kv4.2 increases approximately twofold between P5 and P20, and the increase in Kv4.2 expression appears to be complete by P20 (Fig. 8, *lower right*). Similar to the findings with Kv1.2, therefore, the developmental expression of the Kv4.2 protein closely parallels the observed increase in Kv4.2 mRNA (Fig. 6).

A specific protein band at 75 kD is recognized by the anti-Kv1.5 antibody in developing adult rat ventricular membranes (Fig. 7, *upper right*). This band is eliminated when the antibody is preincubated with the fusion protein (Takimoto et al., 1994; Barry et al., 1995; Maletic-Savatic et al., 1995) against which the antibody was generated (Barry et al., 1995). There are also two low molecular weight bands identified in Western blots with

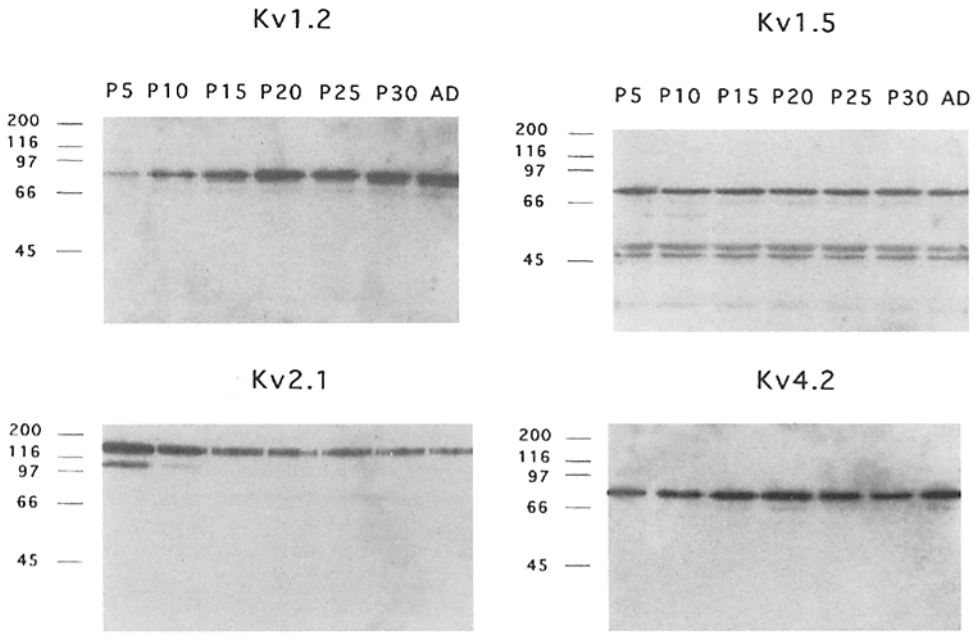

FIGURE 7. Westerns blots reveal marked differences in the postnatal expression patterns of the Kv1.2, Kv1.5, Kv2.1, and the Kv4.2 proteins. Ventricular membrane proteins prepared from P5, P10, P15, P20, P25, P30, and adult animals were fractionated on SDS-Page gels, transferred to PVDF membranes (see MATERIALS AND METHODS) and immunoblotted with the anti-Kv1.2 (*upper left*), anti-Kv1.5 (*upper right*), anti-Kv2.1 (*lower left*), or anti-Kv4.2 (*lower right*) antibodies. To facilitate quantification of subunit expression, 20 μg of ventricular membrane proteins prepared from the hearts of P5, P10, P15, P20, P25, P30, or adult animals were loaded onto each gel. All antibodies were used at a concentration of 1:100 except Kv4.2, which was used at 1:500. Bound antibodies were detected using a chemiluminescence assay (see MATERIALS AND METHODS)

anti-Kv1.5 (Fig. 7, *upper right*); these bands appear to reflect nonspecific binding, as evidenced by the fact that they are not eliminated by preincubation of the antibody with the fusion protein against which the antibody was generated (data not shown). Quantification of Western blots using the anti-Kv1.5 antibody confirmed that the level of Kv1.5 protein expression does not vary appreciably during postnatal development (Fig. 8, *upper right*). In contrast to the findings with Kv1.2 and Kv4.2, therefore, Kv1.5 protein levels do not vary in parallel with the observed developmental increases in Kv1.5 mRNA (Fig. 6). This discrepancy between the protein and the mRNA data suggests post-transcriptional regulation of Kv1.5.

The anti-Kv2.1 antibody specifically labels a single protein band at 130 kD in adult rat ventricular membranes (Barry et al., 1995). Interestingly, and as clearly illustrated in Fig. 7, there are two bands recognized by the anti-Kv2.1 antibody in the P5 and P10 membrane preparations, one at 130 kD and the second at 110 kD; only the 130 kD band is detected at later ages. Both the 130- and the 110-kD bands reflect specific labeling as evidenced by the fact that both bands are eliminated when the antibody was preincubated with the fusion protein (Trimmer, 1991) against which the antibody was generated (data not shown). In addition, the 110-kD band is prominent in ventricular membranes isolated at P0 (data not shown). These findings suggest that there are two distinct isoforms of Kv2.1 in the heart and that expression of these is developmentally regulated (see DISCUSSION). Quantification of the 130-kD band revealed a threefold decrease in Kv2.1 between P5 and P15; the level of Kv2.1 is invariant at later ages (Fig. 8). The variation in the Kv2.1 protein level during postnatal development, therefore, is directly opposite to the observed developmental changes in Kv2.1

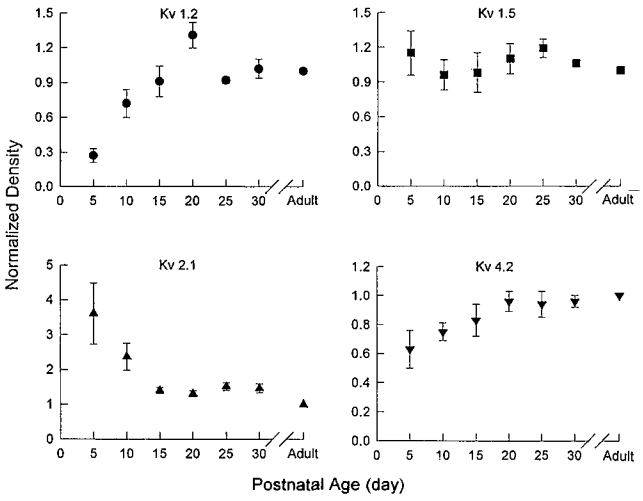

FIGURE 8. Changes in Kv α subunit expression patterns during postnatal development are distinct. Western blots of ventricular membrane proteins were completed as described in the legend of Fig. 7. Films were scanned directly into a Molecular Dynamics densitometer using Image Quant. The density of each band was measured and subsequently normalized to the density of the corresponding band in the adult sample on the same gel. For the Kv2.1 blots, only the high molecular weight band (130 kD) was included in the analyses. Mean (±SEM) values from three to six separate determinations are plotted.

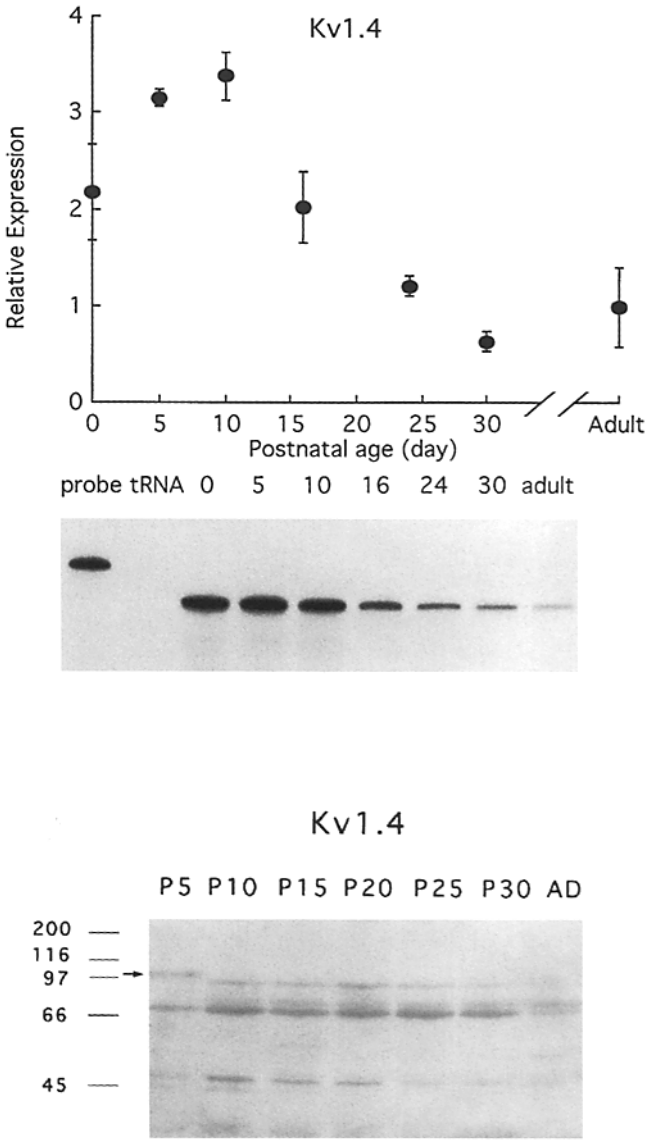

FIGURE 9. The levels of Kv1.4 message and protein decrease markedly and in parallel during postnatal development. In the upper panel, the relative level of Kv1.4 mRNA expression in rat ventricles at various developmental ages is plotted. The data points are the means (±SEM) of four to six separate determinations; in each determination, the data were normalized to the adult value which was set equal to unity. A sample RNase protection assay is shown beneath the plot of the mean data. In the lower panel, Western blots of ventricular membrane proteins (20 μg) isolated at various developmental ages using the anti-Kv1.4 antibody (at 1:200) are displayed. Kv1.4, although readily detected in the P5 sample (*arrow*), is not evident at later ages.

mRNA levels (Fig. 8), suggesting posttranscriptional regulation of Kv2.1.

Developmental Expression of Kv1.4

Interestingly, and in sharp contrast to the findings with the other four subunits, RNase protection assays revealed that Kv1.4 message levels decrease during postnatal development (Fig. 9, *top*). In parallel with the decline in Kv1.4 message, there is a marked decrease in the level of the Kv1.4 protein during the same developmental period (Fig. 9, *bottom*). A very faint band was detected at 97 kD in the P5 sample with the anti-Kv1.4 antibody at a much lower dilution (1:200) than those (1:500 to 1:1,000) that we have previously demonstrated reveal robust labeling of a 97-kD band in adult rat brain (but not heart) membranes (Barry et al., 1995). This band was eliminated when the antibody was preincubated with the peptide against which the antibody was generated (data not shown). As also previously demonstrated, these experiments reveal that high concentrations of anti-Kv1.4 labels several other nonspecific bands in Western blots of P5, P10, P15, P20, P25, P30, and adult rat ventricular membrane proteins.

Outward Currents in Rat Ventricular Myocytes Are Insensitive to Dendrotoxins

Interestingly, several members of the *Shaker* subfamily of voltage-gated K^+ channel subunit proteins, including Kv1.2 (Stühmer et al. 1989), have been reported to be sensitive to blockade by nM concentrations of dendrotoxin, K^+ channel toxins isolated from the mamba *Dendroaspis angusticeps* (Castle et al., 1989). To determine if there are dendrotoxin-sensitive K^+ channel sub-

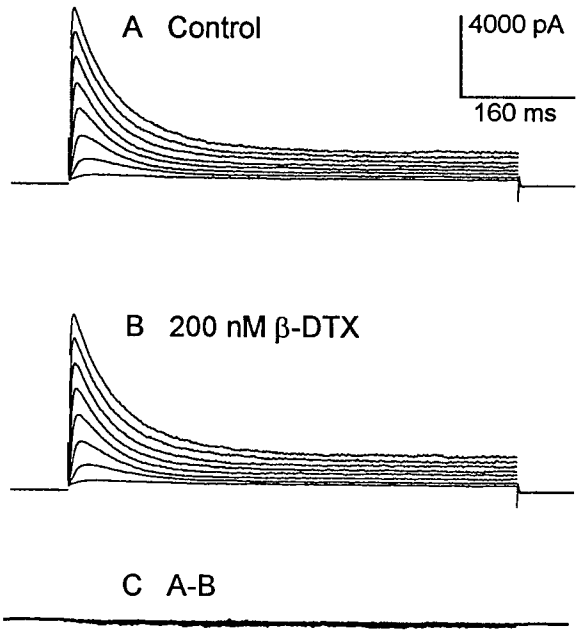

FIGURE 10. Depolarization-activated K^+ currents in rat ventricular myocytes are insensitive to β-dendrotoxin (*β-DTX*). Outward currents were recorded as described in the legend of Fig. 1 in the absence (*A*) and in the presence (*B*) of 200 nM β-DTX. The current records displayed in *C* were obtained by subtraction of the records in the presence of β-DTX (*B*) from the controls (*A*). Similar results were obtained in experiments completed on five other cells.

units that contribute to the formation of the depolarization-activated K^+ channels, I_{to} and I_K, in rat ventricular myocytes, the effects of 20 nM (n = 3) and 200 nM β-dendrotoxin (n = 3) on the voltage-gated K^+ currents in these cells were examined. These experiments revealed no measurable effects of β-dendrotoxin on the depolarization-activated outward K^+ currents in these cells at concentrations up to 200 nM (Fig. 10). The outward K^+ currents recorded in the presence of 200 nM β-dendrotoxin (Fig. 10 *B*) are indistinguishable from the control currents (Fig. 10 *A*) recorded in the same cell. To evaluate toxin efficacy, experiments were also performed on Ltk^- cells transfected with Kv1.2 cDNA (kindly provided by M. Tamkun, Vanderbilt University, Nashville, TN). These experiments revealed that, indeed, nM concentrations of β-, α-, or δ-dendrotoxin reduced the amplitudes of heterologously expressed Kv1.2 currents by >50% (J.M. Nerbonne, unpublished observations). Thus, we conclude that the negative results obtained on rat ventricular myocytes do not reflect a problem with the purity or the activity of the toxins. Rather, we interpret these results as suggesting that there are no voltage-gated K^+ currents in rat ventricular myocytes that are sensitive to the dendrotoxins at concentrations up to 200 nM.

DISCUSSION

Differential Expression of I_{to} and I_K during Postnatal Development

The experiments described here demonstrate that the Ca^{2+}-independent, depolarization-activated outward K^+ currents in rat ventricular myocytes, I_{to} and I_K, develop independently, consistent with previous suggestions that distinct molecular entities underlie the expression of these two conductance pathways (Apkon and Nerbonne, 1991; Barry et al., 1995). I_K density, for example, varies only slightly throughout from postnatal day 5 to the adult; I_{to} density, in contrast, increases more than fourfold during the same developmental period. Qualitatively similar changes in I_{to} density in developing rat ventricular myocytes have been described previously (Kilborn and Fedida, 1990; Wahler et al., 1994), although the increases in I_{to} density reported in the present study are somewhat larger. Also, as suggested previously (Kilborn and Fedida, 1990), the results presented here demonstrate that the time- and voltage-dependent properties of I_{to} do not vary measurably between postnatal day 5 and the adult.

Developmental Expression of Kv1.2, Kv1.4, Kv1.5, Kv2.1, and Kv4.2 mRNAs

The results presented here also demonstrate that the K^+ channel subunits, Kv1.2, Kv1.4, Kv1.5, Kv2.1, and Kv4.2, shown to be expressed at the mRNA level in the adult rat heart (Roberds and Tamkun, 1991*a*, *b*; Dixon and McKinnon, 1994) are also readily detected in developing rat ventricles. In addition, although the expression levels of all five subunits were found to vary during postnatal development, the specific patterns and the time courses of the observed changes are variable. The mRNA levels of four of the five subunits, Kv1.2, Kv1.5, Kv2.1, and Kv4.2, for example, increase with increasing postnatal age. Overall, the largest change was seen for the Kv1.2 mRNA, which increased ~10-fold between birth and the adult. Similar increases in Kv1.2 mRNA levels during postnatal development were reported recently by Nakamura and Iijlma (1994). More modest (approximately three- to fourfold) increases were observed for Kv1.5 and Kv2.1, although for these two subunits, expression reached the adult level at P15 to P20. A threefold increase in Kv4.2 mRNA was also documented, although for this subunit, most of the increase was detected between P15 and the adult. Qualitatively similar results have been reported previously (Roberds and Tamkun, 1991*b*). In sharp contrast to the findings with Kv1.2, Kv1.5, Kv2.1, and Kv4.2, however, we found that Kv1.4 message levels are high at birth (P0), increase between P0 and P10, and subsequently decrease to very low levels in adult ventricles. Although these findings are in direct conflict with at least one previous report using Northern analysis (Roberds and Tamkun, 1991*b*), a more recent study using quantitative reverse transcription also found that the Kv1.4 message is much more abundant in neonatal than in adult rat ventricles (Matsubara et al., 1993), consistent with the findings here.

Developmental Expression of Kv1.2, Kv1.4, Kv1.5, Kv2.1, and Kv4.2 Proteins

Previously, we demonstrated that the Kv1.2, Kv1.5, Kv2.1, and Kv4.2 subunits are readily detected in adult rat ventricular membranes whereas Kv1.4 was barely detectable (Barry et al., 1995). The results presented here confirm these previous findings and, in addition, demonstrate that the expression patterns of these subunits vary in distinct ways during postnatal development. The level of the Kv1.2 protein, for example, increases markedly between P5 and P20 in parallel with the increase in Kv1.2 mRNA. The Kv4.2 protein also increases during this period, albeit to a smaller extent than Kv1.2. The expression patterns of Kv1.5 and Kv2.1, however, are quite distinct: Kv1.5 protein levels are invariant throughout postnatal development, and Kv2.1 protein levels decrease. These findings suggest posttranscriptional regulation of Kv1.5 and Kv2.1, but not of Kv1.2 or Kv4.2, expression. Interestingly, there are also two isoforms of the Kv2.1 protein in early (≤P10) rat ventricles, whereas in older

animals only a single Kv2.1 species is evident. These differences may reflect the expression of two splice variants of Kv2.1 in neonatal ventricles or, alternatively, developmentally regulated posttranslational modifications (Trimmer, 1993) of this subunit. Further experiments will be necessary to distinguish between these possibilities.

In contrast to the findings for the other four subunits, the Kv1.4 protein was barely detectable in rat ventricles throughout postnatal development; a weak signal was detected with the anti-Kv1.4 antibody in P5 ventricular membranes. It seems unlikely that the weak/absent signals with this antibody on Western blots of ventricular membrane proteins reflects the experimental conditions used because all of the other antibodies gave unambiguous results. In addition, the anti-Kv1.4 antibody works well in Westerns of rat brain membrane proteins (Sheng et al., 1993; Barry et al., 1995). The apparent absence of Kv1.4 in membranes prepared from P10 to adult ventricles, therefore, cannot be explained by problems with the antibody or with the methods in general. Rather, we suggest that Kv1.4 is not an abundant protein in ≥P10 rat ventricles and, further, that this subunit likely does not play an important role in the formation of functional depolarization-activated K^+ channels in rat ventricular myocytes.

Relationship between K^+ Channel α Subunits and Functional K^+ Channels in Ventricular Myocytes

A goal of the experiments here was to provide further insights into the likely subunits that underlie rat ventricular I_{to} and I_K channels. Previously, we suggested that, of the subunits expressed, Kv2.1 seemed the most likely candidate for I_K primarily because heterologous expression of Kv2.1 reveals slowly activating, TEA-sensitive K^+ currents (Frech et al., 1989) similar to I_K (Apkon and Nerbonne, 1991). Heterologous expression of Kv4.2 (Baldwin et al., 1991; Blair et al., 1991), Kv1.2 (Paulmichl et al., 1991), or Kv1.5 (Stühmer et al., 1989), in contrast, yields rapidly activating K^+ currents that are sensitive to 4-AP and relatively insensitive to TEA. Also, expressed Kv1.2 currents are sensitive to nM concentrations of DTX (Stühmer et al., 1989), whereas I_K in rat ventricular myocytes is insensitive to DTX (Fig. 10). If the hypothesis that Kv2.1 underlies I_K is correct, then one might have expected that Kv2.1 expression, like I_K density, would change little during postnatal development. The experiments here, however, revealed that Kv2.1 protein levels decrease markedly during postnatal development. These results suggest either that Kv2.1 does not play a role in the generation of I_K channels or, alternatively, that the number of functional I_K channels is highly regulated by posttranslational mechanisms. Further experiments are necessary to distinguish between these possibilities.

Previously, we also suggested that Kv4.2, rather than Kv1.4, likely underlies rat ventricular I_{to} primarily because this subunit is abundant in rat ventricles at both the message (Dixon and McKinnon, 1994) and protein (Barry et al., 1995) levels and because expression of Kv4.2 (Baldwin et al., 1991; Blair et al., 1991) in *Xenopus* oocytes reveals transient K^+ currents that are similar to I_{to} (Apkon and Nerbonne, 1991). In addition, Kv4.2 mRNA expression varies through the thickness of the ventricular wall (Dixon and McKinnon, 1994) in a manner analogous to the variation in I_{to} density (Clark et al., 1993). Although the results here are consistent with a role for Kv4.2 in the formation of I_{to} channels, the (fourfold) increase in I_{to} density between P5 and P30 is larger than that expected based on Kv4.2 protein expression patterns (if one assumes that there should be a direct relationship between protein levels and channel densities). One interesting possibility to consider is that there are accessory β subunits associated with Kv4.2 in vivo and that these function to increase the density of functional I_{to} channels, analogous to the role ascribed to β subunits of L type, voltage-gated Ca^{2+} channels (DeWaard et al., 1994). Biochemical studies have demonstrated that there are accessory β subunits of brain voltage-gated K^+ channels of the *Shaker* (Muniz et al., 1992) and *Shab* (Trimmer, 1991) subfamilies, and several *Shaker* subfamily β subunits have now been cloned from brain (Rettig et al., 1994) and heart (England et al., 1995*a*, *b*; Majumder et al., 1995; Morales et al., 1995). Although there is no direct evidence for β subunits of the *Shal* subfamily, it has been shown that coexpression of low molecular weight brain poly(A)$^+$ RNA with Kv4.1 (or Kv4.2) modulates the properties and the densities of functional Kv4.1 (or Kv4.2) channels (Chabala et al., 1993; Serôdio et al., 1994), consistent with the expression of an accessory subunit. Further experiments will be necessary to explore the possibility that there are β subunits that associate with Kv4.2 in the heart.

The finding that Kv1.2 is also abundant in adult rat ventricle and that the expression of this subunit increases during postnatal development in parallel with the increase in I_{to} density suggests that Kv1.2 (either alone or in combination with Kv1.5 and/or a β subunit) should also be considered a candidate for I_{to}. Heterologous expression of Kv1.2, however, yields rapidly activating, very slowly inactivating K^+ currents with properties quite different from rat ventricular I_{to} (Paulmichl et al., 1991). The strongest argument against a role for Kv1.2 is that heterologously expressed Kv1.2 currents are sensitive to nM concentrations of DTX (Castle et al., 1989), whereas DTX at concentrations up to 200 nM has no effect on I_{to} (or I_K) in rat ventricular myocytes (Fig. 10). Nevertheless, it is certainly possible that Kv1.2 contributes to rat ventricular I_{to} and that the

DTX binding site is rendered inaccessible by association with Kv1.5 and/or a β subunit or possibly as a result of posttranslational processing. Although we favor the hypothesis that Kv4.2 underlies I_{to}, it is clear that alternative experimental strategies will be necessary to explore directly the roles of Kv4.2 and Kv1.2 (alone or in combination with Kv1.5 and/or a β subunit) in the formation of functional I_{to} channels.

Summary

The analysis of the developmental expression voltage-gated K^+ channel currents and Kv α subunits completed here has revealed that the I_{to} and I_K develop independently in rat ventricular myocytes, consistent with previous suggestions that distinct molecular entities underlie these two conductance pathways (Apkon and Nerbonne, 1991; Barry et al., 1995). In addition, the finding that the time- and voltage-dependent properties of the currents do not change measurably suggests that the molecular compositions of functional I_{to} and I_K channels are the same from postnatal day 5 to adult. The biochemical studies completed here, however, have not provided clear insight into the Kv α subunits that contribute to functional I_{to} and/or I_K channels. Rather, these analyses have revealed that, throughout postnatal development there is a mismatch between the numbers of Kv α subunits and functional voltage-gated K^+ channels expressed, if we assume that Kv α subunits in different subfamilies do not combine, as has been demonstrated for Kv α subunits in heterologous systems (Covarrubias et al., 1991). We recognize that it might be suggested that the discrepancy between the biochemical and electrophysiological data reflects contamination from cell types other than ventricular myocytes in the biochemical studies. This possibility seems quite unlikely, however, because we have previously demonstrated that Kv α subunit expression patterns in Western blots of membrane proteins prepared from whole ventricles and isolated myocytes are indistinguishable (Barry et al., 1995). Thus, although we still favor the hypotheses (above) concerning the roles of Kv2.1 and Kv4.2 in the formation of functional I_K and I_{to} channels, it is clear that alternative experimental strategies must be applied to test these hypotheses directly, as well as to define the functional roles of Kv1.2 and Kv1.5. These must involve identifying and exploiting K^+ channel toxins that specifically target Kv2.1 or Kv4.2, as well as molecular approaches focussed on manipulating Kv α subunit expression directly and assessing the functional consequences of these manipulations.

Finally, it is important to emphasize that the studies described here have also revealed clear mismatches between Kv α subunit expression at the mRNA and protein levels (most notably for Kv1.5 and Kv2.1). These findings clearly suggest that there are posttranscriptional mechanisms in place for regulating Kv α subunit expression (at least for Kv1.5 and Kv2.1). These observations emphasize the need to proceed cautiously when attempting to draw conclusions about the expression of functional channels based on analyses of changes in message levels alone.

In Memoriam: This work is dedicated to the memory of our former colleague, collaborator and friend, John P. Merlie, who died suddenly and unexpectedly on May 27, 1995.

We thank Drs. Morgan Sheng and Lily Y. Jan for providing us with anti-Kv1.2, anti-Kv1.4, and anti-Kv4.2 antibodies, and Dr. Michael M. Tamkun for providing the Kv1.2 - L*tk*$^-$ cell line.

This work was supported by grants from the Monsanto-Searle/Washington University Biomedical Research Program (J.M. Nerbonne) and the National Institutes of Health (J.M. Nerbonne and D. McKinnon) and the Council for Tobacco Research (J.S. Trimmer). J.S. Trimmer is an Established Investigator of the American Heart Association; D.M. Barry is the recipient of a predoctoral fellowship from the American Heart Association, Missouri Affiliate.

Original version received 14 May 1996 and accepted version received 31 July 1996.

REFERENCES

Anumonwo, J.M.B., L.C. Freeman, W.M. Kwok, and R.S. Kass. 1991. Potassium channels in the heart: electrophysiology and pharmacological regulation. *Cardiovasc. Drug Rev.* 9:299–316.

Apkon, M., and J.M. Nerbonne. 1991. Characterization of two distinct depolarization-activated K^+ currents in isolated adult rat ventricular myocytes. *J. Gen. Physiol.* 97:973–1011.

Baldwin, T.J., M.L. Tsaur, G.A. Lopez, Y.N. Jan, and L.Y. Jan. 1991. Characterization of a mammalian cDNA for an inactivating voltage-sensitive K^+ channel. *Neuron.* 7:471–483.

Barry, D.M., and J.M. Nerbonne. 1996. Myocardial potassium channels: electrophysiological and molecular diversity. *Annu. Rev. Physiol.* 58:363–394.

Barry, D.M., J.S. Trimmer, J.P. Merlie, and J.M. Nerbonne. 1995. Differential expression of voltage-gated K^+ channel subunits in adult rat heart: Relationship to functional K^+ channels? *Circ. Res.* 77:361–369.

Blair, T.A., S.L. Roberds, M.M. Tamkun, and R.P. Hartshorne. 1991. Functional characterization of RK5, a voltage-gated K^+ channel cloned from the rat cardiovascular system. *FEBS Lett.* 295:211–213.

Boyle, W.A., and J.M. Nerbonne. 1991. A novel type of depolarization-activated K^+ current in isolated adult rat atrial myocytes. *Am. J. Physiol.* 260:H1236–H1247.

Boyle, W.A., and J.M. Nerbonne. 1992. Two functionally distinct 4-aminopyridine-sensitive outward K^+ currents in adult rat atrial myocytes. *J. Gen. Physiol.* 100:1047–1061.

Castle, N.A., D.G. Haylett, and D.H. Jenkinson. 1989. Toxins in the characterization of potassium channels. *Trends Neurosci.* 12:59–65.

Castle, N.A., and M.T. Slawsky. 1992. Characterization of 4-aminopyridine block of the transient outward K^+ current in adult rat ventricular myocytes. *J. Pharmacol. Exp. Ther.* 264:1450–1459.

Chabala, L.D., N. Bakry, and M. Covarrubias. 1993. Low molecular weight poly(A)$^+$ mRNA species encode factors that modulate gating of a non-*Shaker* A-type K^+ channel. *J. Gen. Physiol.* 102:713–728.

Clark, R.B., R.A. Bouchard, E. Salinas-Stefanson, J. Sanchez-Chalupa, and W.R. Giles. 1993. Heterogeneity of action potential waveforms and potassium currents in rat ventricle. *Cardiovasc. Res.* 27:1795–1799.

Covarrubias, M., A. Wei, and L. Salkoff. 1991. *Shaker, Shal, Shab,* and *Shaw* express independent K^+ current systems. *Neuron.* 7:763–773.

Danielson, P.E., S. Forss-Petter, M.A. Brow, L. Calavetta, J. Douglass, R.J. Milner, and J.G. Sutcliffe. 1988. p1B15: a cDNA clone of the rat mRNA encoding cyclophilin. *DNA (NY).* 7:261–267.

DeWaard, M., M. Pragnell, and K.P. Campbell. 1994. Ca^{2+} channel regulation by a conserved beta subunit domain. *Neuron.* 13:495–503.

Dixon, J.E., and D. McKinnon. 1994. Quantitative analysis of mRNA expression in atrial and ventricular muscle of rats. *Circ. Res.* 75:252–260.

England, S.K., V.N. Uebele, H. Shear, K. Kodali, P.B. Bennett, and M.M. Tamkun. 1995*a*. Characterization of a novel K^+ channel β subunit expressed in human heart. *Proc. Natl. Acad. Sci. USA.* 92: 6309–6313.

England, S.K., V.N. Uebele, H. Shear, K. Kodali, P.B. Bennett, and M.M. Tamkun. 1995*b*. A novel K^+ channel β-subunit (hKvβ1.3) is produced via alternative mRNA splicing. *J. Biol. Chem.* 270: 28531–28534.

Frech, G.C., A.M.J. VanDongen, G. Schuster, A.M. Brown, and R.H. Joho. 1989. A novel potassium channel with delayed rectifier properties isolated from rat brain by expression cloning. *Nature (Lond.).* 340:642–645

Hamill, O.P., A. Marty, E. Neher, B. Sakmann, and F.J. Sigworth. 1981. Improved patch-clamp techniques for high resolution current recording from cells and cell free membrane patches. *Pflüg. Archiv.* 391:85–100.

Kilborn, M.J., and D. Fedida. 1990. A study of the developmental changes in outward currents in rat ventricular myocytes. *J. Physiol. (Lond.).* 430:37–60.

Majumder, K., M. DeBiasi, Z. Wang, and B. Wible. 1995. Molecular cloning and functional expression of a novel potassium channel β subunit from human atrium. *FEBS Lett.* 361:13–16.

Maletic-Savatic, M., N.J. Lenn, and J.S. Trimmer. 1995. Differential spatiotemporal expression of K^+ channel polypeptides in rat hippocampal neurons developing *in situ* and *in vitro*. *J. Neurosci.* 15: 3840–3851.

Matsubara, H., J. Suzuki, and M. Inada. 1993. *Shaker*-related potassium channel, Kv1.4, mRNA regulation in cultured rat heart myocytes and differential expression of Kv1.4 and Kv1.5 genes in myocardial development and hypertrophy. *J. Clin. Invest.* 92: 1659–1666.

Morales, M.J., R.C. Castellino, A.L. Crews, R.L. Rasmusson, and H.C. Strauss. 1995. A novel β subunit increases the rate of inactivation of specific voltage-gated potassium channel α subunits. *J. Biol. Chem.* 270:6272–6277.

Muniz, Z.M., D.N. Parcej, and J.O. Dolly. 1992. Characterization of monoclonal antibodies against voltage-dependent K^+ channels raised using α-dendrotoxin acceptors purified from bovine brain. *Biochemistry.* 31:12297–12303.

Nakamura, K., and T. Iijima. 1994. Postnatal changes in mRNA expression of the K^+ channel in rat cardiac ventricles. *Jpn. J. Pharmacol.* 66:489–492.

Paulmichl, M., P. Nasmith, R. Hellmiss, K. Reed, W.A. Boyle, J.M. Nerbonne, E.G. Peralta, and D.E. Clapham. 1991. Cloning and expression of a cardiac delayed rectifier potassium channel RAK. *Proc. Natl. Acad. Sci. USA.* 88:7892–7895.

Rettig, J., S.H. Heinemann, F. Wunder, C. Lorra, D.N. Parcej, J.O. Dolly, and O. Pongs. 1994. Inactivation properties of voltage-gated K^+ channels altered by presence of β-subunit. *Nature (Lond.).* 369:289–294.

Roberds, S.L., and M.M. Tamkun. 1991*a*. Cloning and tissue-specific expression of five voltage gated potassium channel cDNAS expressed in rat heart. *Proc. Natl. Acad. Sci. USA.* 88:1798–1802.

Roberds, S.L. and M.M. Tamkun. 1991*b*. Developmental expression of cloned cardiac potassium channels. *FEBS Lett.* 284:152–154.

Serôdio, P., C. Kentros, and B. Rudy. 1994. Identification of molecular components of A-type channels activating at subthreshold potentials. *J. Neurophysiol.* 72:1516–1529.

Sheng, M., Y.J. Liao, Y.N. Jan, and L.Y. Jan. 1993. Presynaptic A-current based on heteromultimeric K^+ channels detected *in vivo*. *Nature (Lond.).* 365:72–75.

Sheng, M., M.-L. Tsaur, Y.N. Jan, and L.Y. Jan. 1992. Subcellular segregation of two A-type K^+ channel proteins in rat central neurons. *Neuron.* 9:271–284.

Sheng, M., M.-L. Tsaur, Y.N. Jan, and L.Y. Jan. 1994. Contrasting subcellular localization of the Kv1.2 K^+ channel subunit in different neurons of rat brain. *J. Neurosci.* 14:2408–2417.

Stühmer, W., J.P. Ruppersberg, K.H. Schröter, B. Sakmann, M. Stöcker, K.P. Giese, A. Perschke, A. Baumann, and O. Pongs. 1989. Molecular basis of functional diversity of voltage-gated potassium channels in mammalian brain. *EMBO (Eur. Mol. Biol. Organ.) J.* 8:3235–3244.

Takimoto K., A.F. Fomina, R. Gealy, J.S. Trimmer, and E.S. Levitan. 1993. Dexamethasone rapidly induces Kv1.5 K^+ channel gene transcription and expression in clonal pituitary cells. *Neuron.* 11: 359–369.

Takimoto, K., and E.S. Levitan. 1994. Glucocorticoid induction of Kv1.5 K^+ channel gene expression in ventricle of rat heart. *Circ. Res.* 75:1006–1013.

Trimmer, J.S. 1991. Immunological identification and characterization of a delayed rectifier K^+ channel polypeptide in rat brain. *Proc. Natl. Acad. Sci. USA.* 88:10764–10768.

Trimmer, J.S. 1993. Expression of Kv2.1 delayed rectifier K^+ channel isoforms in the developing rat brain. *FEBS Lett.* 324:205–210.

Tseng-Crank, J.C.L., G.N. Tseng, A. Schwartz, and M.A. Tanouye. 1990. Molecular cloning and functional expression of a potassium channel cDNA isolated from a rat cardiac library. *FEBS Lett.* 268:63–68.

Varro, A., D.A. Lathrop, S.B. Hester, P.P. Nanasi, and J.G.Y. Papp. 1993. Ionic currents and action potentials in rabbit, rat, and guinea pig ventricular myocytes. *Basic Res. Cardiol.* 88:93–102.

Wahler, G.M., S.J. Dollinger, J.M. Smith, and K.L. Flemal. 1994. Time course of postnatal changes in rat heart action potential and in transient outward current is different. *Am. J. Physiol.* 267: H1157–H1166.